Full-Length Influenza Hemagglutinin HA_2 Refolds into the Trimeric Low-pH-Induced Conformation†

Susanne E. Swalley,*,‡,§ Brian M. Baker,§,|| Lesley J. Calder,⊥ Stephen C. Harrison,‡ John J. Skehel,⊥ and Don C. Wiley§,#

Department of Biological Chemistry and Molecular Pharmacology, Howard Hughes Medical Institute, Harvard Medical School, 250 Longwood Avenue, Boston, Massachusetts 02115, Department of Molecular and Cellular Biology, Howard Hughes Medical Institute, Harvard University, 7 Divinity Avenue, Cambridge, Massachusetts 02138, and National Institute for Medical Research, The Ridgeway, Mill Hill, London NW7 1AA, United Kingdom

Received January 27, 2004; Revised Manuscript Received March 16, 2004

ABSTRACT: The influenza virus uses hemagglutinin (HA) to fuse the viral and cellular membranes. As part of an effort to study the membrane-interacting elements of HA, the fusion peptide, and the C-terminal transmembrane anchor, we have expressed in *Escherichia coli* the full-length HA_2 chain with maltose-binding protein fused at its N-terminus. The chimeric protein can be refolded in vitro in the presence of specific detergents to yield stable, homogeneous trimers, as determined by analytical ultracentrifugation. The trimers have the so-called "low pH" conformation—the rearranged HA_2 conformation obtained when intact HA_1/HA_2 is induced to refold by exposure to low pH—as detected by electron microscopy and monoclonalantibody reactivity. These results provide further evidence for the notion that the neutral-pH structure of intact HA is metastable and that binding of protons lowers the kinetic barriers that prevent rearrangement to the minimum-free-energy conformation. The refolded chimeric protein described here is a suitable species for undertaking studies of how the fusion peptide inserts into membranes and assessing the nature of possible intermediates in the fusion process.

To enter target cells, enveloped viruses such as influenza, human immunodeficiency virus-1 (HIV-1),[1] and Ebola use specific surface glycoproteins to fuse the viral membrane with the target cellular membrane (*1*−*3*). Influenza virus hemagglutinin (HA), the most extensively characterized membrane fusion protein, is a homotrimeric type I transmembrane protein. Each 70-kDa subunit contains two disulfide-linked polypeptide chains, HA_1 and HA_2, created by the proteolytic cleavage of the precursor protein HA_0 (Figure 1) (*4*). This cleavage event is a prerequisite for membrane fusion (*4*). During membrane fusion, the HA binds virus to sialic acid receptors on the cell surface, and following endocytosis the acidic pH (pH 5−6) of endosomal compartments induces dramatic and irreversible reorganization of the HA structure (*5*−*9*).

The HA_2 chain contains two membrane-interacting hydrophobic peptide sequences: an N-terminal "fusion peptide" (residues 1−23), which interacts with the target membrane bilayer (*10*), and a C-terminal transmembrane segment that passes through the viral membrane. Crystallographic studies of the HA ectodomain, both in its nonactivated conformation and in the low-pH-induced state (BHA and $TBHA_2$, Figure 1) suggest that the reorganization of HA_2 moves the fusion peptide from the interior of the neutral-pH structure approximately 100 Å toward the target membrane in the low-pH structure (*7*, *9*). In this process, the middle of the original long α-helix unfolds to form a reverse turn, jackknifing the C-terminal half of the long α-helix backward toward the N-terminus. These molecular rearrangements place the N-terminal fusion peptide and the C-terminal transmembrane (TM) anchor at the same end of the rod-shaped HA_2 molecule (*11*, *12*), facilitating membrane fusion by bringing the viral and cellular membranes together. Structural similarities between the low-pH form of HA_2 and the ectodomains of other viral membrane fusion proteins in their postfusion states suggest that this juxtaposition of termini is a common mechanism for membrane fusion (*1*).

Expression of HA_2 ectodomain residues 23−185 (EHA_2, Figure 1) in *Escherichia coli* results in a soluble trimer of HA_2 with a structure at pH 7 essentially identical to that of

† The research was supported by the Medical Research Council (U.K.), the National Institutes of Health (Grant AI-13654), and the Howard Hughes Medical Institute (HHMI). S.E.S. was supported by a Damon Runyon Cancer Research Foundation Fellowship, DRG-1535, and a Charles A. King Trust Fellowship. S.C.H. and D.C.W. are investigators of the Howard Hughes Medical Institute.

* To whom correspondence should be addressed. E-mail: swalley@crystal.harvard.edu. Phone: 617-432-5602. Fax: 617-432-5600.

‡ Harvard Medical School.

§ Harvard University.

⊥ National Institute for Medical Research.

|| Current address: Department of Chemistry and Biochemistry, University of Notre Dame, 251 Nieuwland Science Hall, Notre Dame, IN 46556.

Deceased.

[1] Abbreviations: HA, hemagluttinin; HA_1, the receptor-binding chain of HA; HA_2, the fusion domain of HA; MBP, maltose binding protein; MHA_2, MBP linked to full-length HA_2 (residues 1−221); BHA, soluble neutral-pH HA; $TBHA_2$, trimeric BHA_2 fragment; EM, electron microscopy; mAb, monoclonal antibody; EDTA, ethylenediaminetetraacetic acid; IPTG, isopropyl-D-thiogalactopyranoside; ABTS, 2,2′-azinobis(3-ethylbenzothiazoline-6-sulfonic acid); SDS, sodium dodecyl sulfate; PAGE, polyacrylamide gel electrophoresis; PBS, phosphate-buffered saline.

10.1021/bi049807k CCC: $27.50
Published on Web 04/27/2004

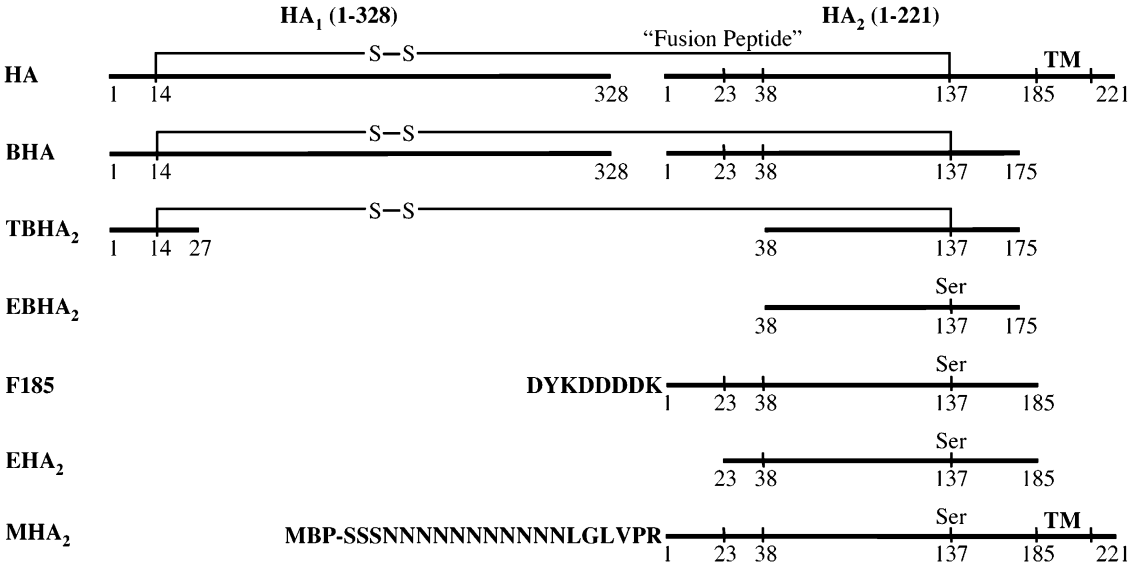

FIGURE 1: Schematic structure of influenza virus HA and various truncations. MHA_2 (MBP linked to HA_2 1−221) is the protein described here. BHA and $TBHA_2$ are ectodomain fragments of HA obtained from virus. $EBHA_2$, F185, EHA_2, and MHA_2 are expressed in *E. coli*. Abbreviations: TM, transmembrane anchor; S−S, interchain disulfide bond from HA_1 Cys-14 to HA_2 Cys-137.

$TBHA_2$, the fragment derived from viral HA_1/HA_2 by proteolysis following exposure to low pH (*13*, *14*). The structural identity between $TBHA_2$ and EHA_2 suggests that the low-pH-induced conformation of HA_2 is a minimum-energy state, because it forms spontaneously at neutral pH when the protein folds in the absence of HA_1. Moreover, the irreversible conformational change of HA_2 can also be induced by either temperature or urea, and the postfusion state melts at a higher temperature than does the prefusion state (*6*, *15*). These data all support the notion that neutral-pH HA is metastable and that the pH change removes kinetic barriers that prevent premature display of the fusion peptide, leading to either nonproductive aggregation or fusion.

Less is known about how the fusion peptide interacts with membranes during the fusion process. There are a number of conserved residues within the fusion peptide, indicating that its structure within the membrane is likely important to the fusion process (*16*−*18*). Structural studies of pH-activated full-length HA have not been successful, because of aggregation induced by the hydrophobic fusion peptides (*4*), and structural studies of the fusion peptide have been limited to segments of the fusion peptide alone, out of the context of the full-length protein (*19*). Multiple studies have demonstrated that the fusion peptide alone can fuse membranes in vitro, with dependence on specific lipid composition (*20*−*22*). A recent NMR and EPR study by Han and Tamm on residues 1−20 fused to a charged tag in dodecylphosphocholine (DPC) micelles showed the peptide in a kinked conformation with the bend occurring around Asn 12 (*19*). On the basis of these peptide structures, a "spring-loaded boomerang" fusion mechanism has been proposed, in which the kinked shape of the fusion peptide helps induce curvature of the target cell membrane and thus helps initiate membrane fusion (*23*). This proposal remains to be tested structurally in the context of the full-length protein.

The contribution of the TM anchor to fusion is also not fully understood, although a number of studies have suggested that the main role of the TM anchor is to promote the hemifusion to fusion transition (*24*−*28*). Studies on the TM anchor have shown that substitution of this domain and the cytoplasmic tail with glycosylphosphatidylinositol (GPI) results in a trimeric molecule that induces only hemifusion of the membranes (*24*). TM regions from other viral fusion proteins as well as from unrelated type I transmembrane proteins can be substituted for the TM domain of HA without affecting fusion (*25*−*27*). Additionally, Armstrong and White identified that the minimal required length of the TM domain for fusion is 17 amino acids, suggesting that the role of the HA in fusion requires the TM region to span the membrane (*28*). However, there may be a requirement for a specific structural motif, as a single point mutation G520L in the HA_2 transmembrane domain of the Japan/305/57 HA subtype abolishes fusion (*27*).

Biochemical and structural studies of full-length HA_2 could add to an understanding of the structure and function of the lipid-interacting components of HA and provide information on the nature of possible intermediates in the fusion process. We report here the recombinant expression of MHA_2, which corresponds to full-length HA_2 tagged with maltose-binding protein (MBP). The chimeric protein can be refolded in the presence of specific detergents and is shown by analytical ultracentrifugation, electron microscopy, and immunoassays to be both trimeric and in the low-pH form.

EXPERIMENTAL METHODS

Cloning of MHA_2. The construct was cloned into the vector pLM1, which contains a T7 promoter, using a three-part seamless ligation strategy that links the two protein subunits by Ser(3)Asn(11)LeuGlyLeuValProArg. DNA encoding HA_2 residues 1−221 was cloned from the cDNA of the influenza A virus strain X31. The MBP segment was amplified from pMAL-c2x (New England Biolabs). To achieve high levels of bacterial expression and to prevent improper disulfide formation, residues 80−170 were swapped with the same residues from the previously described $EBHA_2$ (HA_2-38−175) (*14*). This segment of HA_2 contains changes in three rare Arg codons (Arg-123, -124, and -127) and the mutation of Cys-137, which forms a disulfide bond with HA_1 residue 14, to Ser. The resultant construct was named MHA_2c. The

normally palmitoylated C-terminal cytosolic cysteines (Cys-210, -217, and -220) were mutated to Ser using the Quickchange method (Stratagene). Additionally, the transmembrane cysteines (Cys-195 and Cys-199) were mutated to Ser and Ala, respectively, resulting in the final construct MHA_2 (MBP-HA_2-(1−221)).

Expression and Purification. The protein was expressed in *E. coli* [BL21(DE3)] cells grown at 37 °C in a rich medium (20 g/L tryptone, 10 g/L yeast extract, 5 g/L NaCl, 20 mL/L glycerol, 50 mM K_2HPO_4, 10 mM $MgCl_2$, 10 g/L glucose, 50 mg/L ampicillin) to an OD_{600} of 1.0. Protein expression was induced with 0.2 mM IPTG, and the cells were grown at 30 °C for 4 h and harvested by centrifugation (1500*g*, 20 min). Cells were lysed by resuspension and sonication in PBS buffer containing 0.2 mg/mL lysozyme, 0.1 mg/mL DNase I, 10 mM $MgCl_2$, Complete protease inhibitor with EDTA (Roche), 1 mM phenylmethylsulfonyl fluoride (PMSF), and 7 μg/mL pepstatin plus detergent. Detergents were screened on a small scale for their ability to solubilize MHA_2 and to allow the MBP subunit to bind the amylose resin (New England Biolabs). All detergents were at concentrations at least 2.5 times above the detergent critical micelle concentration (CMC). Five hundred microliters of induced cells were centrifuged, and lysis buffer was added to the pellet. Following brief sonication, the solution was spun at 16000*g* for 10 min at 4 °C. Amylose resin was prepared by spinning 500 μL of resin at 3000*g* for 5 min, washing once with PBS and then resuspending in 450 μL of PBS. The lysis supernatant was added to the washed resin, and the protein was bound in batch overnight at 4 °C. Following binding, the resin was spun and the supernatant was removed. Samples of the initial lysis, the postbinding supernatant, and the resin were evaluated by SDS−PAGE.

For large-scale preparations, cells were lysed in buffer containing 1% (10× CMC) decyl maltoside (DM). Following centrifugation (12500*g*, 20 min), the supernatant was loaded onto an amylose column at 1 mL/min, and the column was washed with 10 column volumes of PBS containing 0.17% DM (2× CMC), Complete protease inhibitor, and 1 mM PMSF. The protein was eluted with 10 mM maltose in the same buffer, fractions containing MHA_2 were pooled, additional protease inhibitors (0.4 mM Pefabloc SC, Roche, plus 1 μg/mL leupeptin and 0.7 μg/mL pepstatin) were added, and the protein was concentrated to ≥5 mg/mL as measured by OD_{280} of protein diluted with 6 M guanidine-HCl in 0.02 M phosphate pH 6.5 using a calculated extinction coefficient of 107 940 M^{-1} cm^{-1} (*29*). The concentrated protein was frozen in liquid N_2 and stored at −80 °C.

Protein Refolding. The protein was refolded using a method adapted from Garboczi et al. (*30*). First the protein was denatured in 50 mM phosphate pH 8.0 buffer containing 8 M urea, 1% SDS, 100 mM DTT, and 5 mM EDTA, and then the solution was rapidly diluted through a small-gauge (27-1/2) needle into chilled buffer containing 10 mM Tris-HCl (pH 8.0) with 1 M L-arginine, 2 mM EDTA, and detergent on ice. Three detergents were tested for efficient refolding: DM (0.17%, 2× CMC), dodecyl maltoside (DDM, at 0.02 or 0.1%, 2× and 10× CMC, respectively), and β-octyl glucoside (β-OG at 1%, 2× CMC). For large-scale preparations (>20 mg of protein), multiple injections of 10 mg spaced by 1 h gave better results than single injections. The solution was left at 4 °C overnight, then dialyzed 48 h against 10 mM Tris-HCl (pH 8.0) with 0.17% DM (buffer A), with 1 buffer change. Following dialysis, the dilute solution was concentrated by loading it onto a DEAE cellulose anion exchange column (DE52, American Bioanalytical) containing 3 g of resin for every 5 mg of starting protein. The column was washed with 25 mL of buffer A per gram of resin and the protein was eluted with buffer A containing 300 mM NaCl. The protein was further concentrated using a 30 000 MWCO regenerated cellulose concentrator (Amicon) and purified by size-exclusion chromatography on a Superdex 200 column (Pharmacia) in buffer A containing 150 mM NaCl. A final purification was accomplished by diluting the eluted fractions with 10-fold excess of buffer A, loading the diluted protein onto a Mono-Q anion exchange column (MQ 5/5, Pharmacia), and then running a 30-mL gradient of 0−750 mM NaCl, with elution of the trimeric protein at approximately 450 mM NaCl. Refolding of MHA_2c, containing the C-terminal Cys residues, was carried out as above with the addition of 1 mM DTT to all steps.

Detergent Screening. Those detergents that showed good protein solubilization and significant resin binding were tested for the ability to maintain MHA_2 as a trimer. The detergents were exchanged by anion exchange chromatography in the following manner: a small DE-52 column (1 g of resin) was incubated with 0.17% DM in buffer A and loaded with approximately 40 μg of protein. The column was filled with buffer A with 0.17% DM, and then slowly switched to the detergent to be tested. Buffer containing the new detergent was used to wash the column, and then the protein was eluted with 300 mM NaCl in buffer A plus the test detergent. Size-exclusion chromatography was used to determine the stability of the trimer after this process. Proteins were stored at 4 °C for one week and reexamined by size-exclusion chromatography to verify stability of the trimeric form of the protein over time in the new detergent. Concentrations of detergent used (purchased from Anatrace) were 0.2% cyclohexyl pentyl maltoside (Cymal-5), 0.15% cyclohexyl hexyl maltoside (Cymal-6), 1.5% nonyl-phosphocholine (Fos-choline-9), 0.85% heptylcarbamoyl methyl glucopyranoside (HECAMEG), 0.1% undecyl maltoside (UM), 0.025% polyoxyethylene(8) dodecyl ether ($C_{12}E_8$), and 0.4% pentaoxyethylene octyl ether (C_8E_5).

Chemical Cross-Linking. MHA_2 (0.5 mg/mL in 10 μL PBS with 0.17% DM) was cross-linked with bis(sulfosuccinimidyl)suberate (BS^3, Pierce) at room temperature for 30 min and quenched by adding Tris-HCl (pH 6.8) to 50 mM.

Analytical Ultracentrifugation. Sedimentation equilibrium analytical ultracentrifugation (AUC) was performed in a Beckman Optima XL-A analytical ultracentrifuge. Six-channel cells were used, and data were acquired at a resolution of 0.001 cm with five replicates. Absorbance at 280 nm was used to monitor concentration gradients. Samples were determined to have reached equilibrium when scans taken 4 h apart showed no systematic differences. Solvent density was calculated through summation of the contribution of buffer components (*31*). The protein partial specific volume was calculated from the amino acid composition (*32*). In all experiments, multiple datasets at different rotor speeds and/or loading concentrations were analyzed globally, with local parameters for reference concentrations

and baseline offsets and global parameters for the molecular weight. Best-fits were determined through visual inspection of the residuals. Data analysis was performed using the nonlinear least-squares fitting routines in the software package Mathematica (Wolfram Research). Data were fit to equations of the following form:

$$c = c_0 \exp\left(\frac{\omega^2}{RT} M_b (r^2 - r_0^2)\right) + \delta \quad (1)$$

where c_0 is the concentration at a reference position, ω^2 is the angular velocity, RT is the product of the gas constant and the absolute temperature, r is the radial position, r_0 is the reference position, and δ is a baseline offset. M_b in eq 1 is the buoyant molecular weight or the mass of solvent displaced by the sedimenting particle. Errors were propagated using standard techniques (*33*).

Analytical Ultracentrifugation by Varying Solvent Density. Experiments were performed using D_2O to vary solvent density systematically, a technique that allows determination of the molecular weight of protein plus bound detergent, through the dependence of M_b on ρ (*34*, *35*), seen in the following equation:

$$M_b = M(k - \bar{v}\rho) \quad (2)$$

where M is the molecular weight, k is the fractional increase in molecular weight due to proton-deuteron exchange, $\bar{v}$ is the partial specific volume, and ρ is the solvent density. AUC experiments in D_2O were performed at 4 °C using the detergent DM. For the analysis of the DM micelle alone, a 5 mM DM solution (2.8× CMC) was loaded with the hydrophobic dye cibracon blue (final concentration of 5 μM). This solution was diluted to give an absorbance of ~0.2 at 280 nm. Rotor speeds were 19 000, 22 000, and 25 000 rpm. Buffered D_2O solutions of DM were prepared by directly dissolving detergent in the desired of D_2O/buffer solution. Buffer conditions were 10 mM Tris-HCl (pH 8.0) with 150 mM NaCl. As eq 2 has two unknowns (M and $\bar{v}$), a minimum of two determinations of M_b at different solvent densities (D_2O concentrations) is required; we took datasets at four D_2O concentrations (0, 30, 60, and 90%).

For analysis of the protein plus bound detergent, three protein concentrations over the range of 0.12−0.5 mg/mL were used. Rotor speeds were 8500, 9500, 10 500, and 11 500 rpm. Buffer conditions were the same as with the DM micelle alone, except that three D_2O concentrations (0, 40, and 90%) were used. Exchange into buffered D_2O solutions was performed by dialysis for ~24 h against a 10 000 MWCO membrane. Dialysis was performed in tightly sealed containers to minimize the influence of humidity on the D_2O concentration.

Analysis of the density modification experiments was performed by determining the M_b of the sedimenting species by fixing $\bar{v}$ at zero during data fitting. The fractional increase in molecular weight due to proton-deuteron exchange (k) was accounted for by assuming exchange of all DM hydroxyl protons in the case of the DM experiments, or using the value of 1.0155 for proteins in 100% D_2O for the protein + detergent experiments (*34*). The value of k was scaled according to percent D_2O. The values of M_b were likewise corrected for the percentage of D_2O using the correction factor of 1.111 for 100% D_2O (equal to the molecular weight of D_2O over H_2O, scaled by the percentage D_2O). The molecular weight and $\bar{v}$ of the sedimenting species were then determined from eq 2 by solving the resulting simultaneous equations (three for protein plus detergent, six for DM alone) using *Mathematica*. The results are presented as the average plus or minus the standard deviation of all solutions.

Analytical Ultracentrifugation in C_8E_5. Experiments in neutrally buoyant detergent were performed as described by Fleming et al (*36*). The buoyant molecular weight of the sedimenting particle, in this case protein plus bound detergent, can be expressed as the sum of the contributions from the protein and the detergent:

$$M_b = M_p((1 - \bar{v}_p\rho) + n_d(1 - \bar{v}_d\rho)) \quad (3)$$

where M_p is the molecular weight of the protein, $\bar{v}_p$ and $\bar{v}_d$ are the partial specific volumes of the protein and the detergent, respectively, and n_d is the amount of bound detergent. From eq 3, if the product $\bar{v}_d\rho$ is equal to one, the contribution of bound detergent to the buoyant molecular weight is zero. The detergent pentaoxyethylene octyl ether (C_8E_5) is a neutrally buoyant detergent with a $\bar{v}_d$ of 0.993 mL/g at 25 °C (*37*). Experiments were performed at 25 °C. The buffer was 20 mM phosphate (pH 7) with 200 mM NaCl, which has a density of 1.0075 g/mL at 25 °C. Thus, $\bar{v}_d\rho$ is close to one within the precision of the analytical ultracentrifuge. Three concentrations of protein chromatographically exchanged from DM into C_8E_5 were used, spanning the range of 0.12−0.5 mg/mL. Rotor speeds were 7000, 10 000, and 12 000 rpm, for a total of nine datasets.

ELISA Assay. All measurements were done in triplicate and at 22 °C. All washes were carried out with PBST (PBS with 0.05% Tween-20). Using 96-well Maxisorp plates from Nunc, 50 μL of a 1:250 dilution of mouse ascites IIF4 monoclonal antibody, which recognizes the low-pH form of HA_2 (*12*), was incubated overnight at room temperature. The plates were washed 3 times with PBST, blocked for 2 h with 3% BSA with 0.02% sodium azide, and washed with PBST (5 times) to prepare them for protein binding. The protein (MHA_2 or BHA) was diluted (1:300) in either pH 7.4 or pH 5 PBS for 5 min, and then diluted again (to a final of 1:1000) with pH 7.4 PBS and 100 μL added to each well. Approximately 500 ng of each protein was loaded per well. After 2 h, the plates were washed 5 times, and then 100 μL of a 1:1000 dilution of either rabbit anti-HA VACC polyclonal antibody or anti-MBP antiserum (New England Biolabs) was added and the plates were incubated for 1 h. The plates were washed and a 1:10 000 dilution of goat anti-rabbit horseradish peroxidase (Sigma) was added. After 1 h, the plate was washed 5 times, ABTS (Roche) was added, and absorption readings were taken at 410 nm in a Dynatech MR4000 plate reader. Absorption intensities were normalized to the strongest absorption on the plate, and at least two separate experiments (a minimum of six replicates) were used for each numerical determination.

Electron Microscopy. Samples were absorbed to carbon-coated grids and negatively stained with 1% sodium silicotungstate (pH 7). For antibody-labeling experiments, LC89, a monoclonal antibody that binds low-pH HA_2 between residues 106−112 (*12*), was incubated with MHA_2 prior to coating the grids. The grids were viewed with a JEOL

1200EX microscope operated at 100 kV under minimum dose and accurate defocus conditions.

RESULTS AND DISCUSSION

Full-Length HA_2 Can Be Produced Recombinantly. Initial attempts to express full-length HA_2(1−221) with either a FLAG or a 6xHis tag on the N-terminus showed little or no protein expression in a standard *E. coli* expression system (data not shown), even though a truncated trimeric HA_2(1−185) lacking the TM domain and with a FLAG tag at the N-terminus had been expressed previously (F185, Figure 1) (*38*). Studies have demonstrated that proteins fused to an N-terminal MBP moiety have increased solubility and expression (*39*, *40*). In particular, MBP has been shown to solubilize the trimeric gp21 ectodomain from human T cell leukemia virus type 1, and its three-dimensional structure was determined to a resolution of 2.5 Å (*41*). We attached MBP to the N-terminus of full-length HA_2 (construct MHA_2c), and then eliminated the five C-terminal cysteines present in the TM and cytosolic domains of HA_2 (Cys-195, -199, -210, -217, and -220). The three cytosolic cysteines (Cys-210, -217, and -220), which are normally palmitoylated in mammalian cells, were mutated to serine, a change that does not affect the fusogenic ability of HA (*42*). The nonconserved Cys-195 and Cys-199 were mutated to serine and alanine, respectively, based on sequence alignment with 15 hemagglutinin subtypes. The resultant construct, MHA_2, is expressed at high levels in *E. coli* (Figure 2a, lane 1).

Whether a particular membrane protein will reconstitute functionally into detergent micelles must be determined empirically. We examined 19 different detergents for their ability to solubilize the MHA_2 construct during cell lysis and allow for binding to the amylose affinity column (see Supporting Information). Ten detergents met these criteria. However, despite the fact that the protein's MBP moiety is capable of binding the amylose resin, size-exclusion chromatography on the purified protein showed it to be a soluble aggregate (data not shown). Nominé et al. observed similar soluble aggregates with a fusion protein of MBP with human papilloma virus E6, and they proposed that the chimera forms a protein micelle, with the misfolded E6 protein buried away from solvent and the correctly folded MBP molecules exposed to the solvent (*43*). It is likely that this phenomenon occurs with the MHA_2 construct as well, as with virion HA in the absence of detergent. High yields of pure aggregate, between 40 and 60 mg per liter of bacterial culture, can be obtained using DM in the lysis buffer (Figure 2A, lane 4).

We produced soluble trimeric MHA_2 by denaturing the soluble aggregate and refolding the protein by rapid dilution into a solution containing 0.17% DM (2× CMC). Since preliminary refolding experiments of a construct containing the 5 C-terminal Cys residues (construct MHA_2c) showed a predominance of incorrectly disulfide-linked protein, we chose to work exclusively with the MHA_2 construct. Several denaturant solutions were tested, and the highest refolding yield was achieved with 8 M urea and 1% SDS. Following refolding, dialysis, and concentration, the trimeric protein can be purified by size-exclusion chromatography (Figure 2A, lane 6, and Figure 2B). The main peak can be effectively separated away from aggregate by a Mono-Q anion exchange column (Figure 2C). The yield for MHA_2 refolded in the

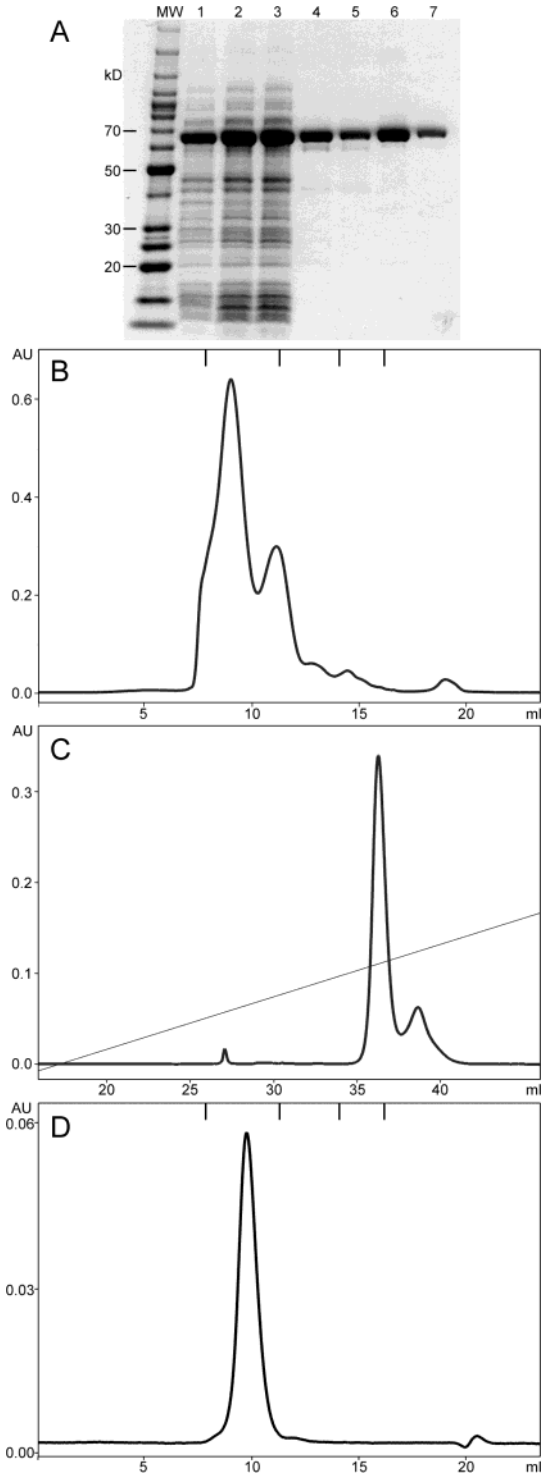

FIGURE 2: Expression, purification, and refolding of MHA_2. (A) SDS−PAGE (4−20% gradient gel) of MHA_2. Lane 1, BL21(DE3) cells after 4 h of induction; lane 2, supernatant after lysis and centrifugation; lane 3, flow-through from the amylose affinity column; lane 4, eluate from the amylose column; lane 5, MHA_2 after refolding, prior to FPLC purification; lane 6, pooled trimeric MHA_2 after size-exclusion chromatography; lane 7, pooled MHA_2 after final anion exchange column. (B) Size-exclusion chromatograph after refolding. Hashmarks indicate location of molecular weight standards (670, 158, 44, and 17 kDa, from left to right). (C) Final purification step by anion exchange chromatography. The main peak represents trimeric MHA_2, while the adjacent peak is aggregated protein. (D) Chromatograph of the main peak from panel C rerun on a size-exclusion column, demonstrating that the purified trimer remains a single species and does not reaggregate significantly. Hashmarks are the same as in panel B.

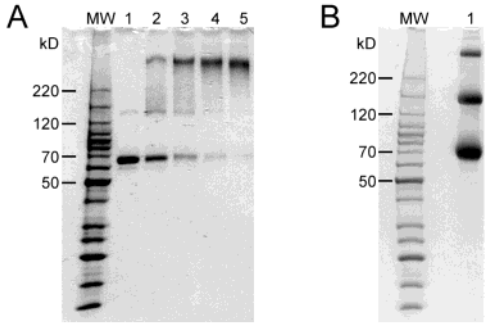

FIGURE 3: (A) SDS−PAGE (4−20% gradient gel) of chemically cross-linked MHA_2 under reducing conditions. Lanes 1−5, MHA_2 with cross-linking reagent BS^3 at 0, 0.1, 0.25, 0.5, and 1.0 mM, respectively. (B) SDS−PAGE (4−20% gradient gel) of unreduced, full-length HA, no cross-linking reagent.

presence of DM ranges from 4 to 10%, resulting in a final yield of 2−5 mg/L of original bacterial culture. Figure 2D shows the pure protein rerun over a size-exclusion column, now as a single symmetric peak with an apparent molecular weight of approximately 350 kDa for the protein plus micelle, which is larger than the calculated molecular weight of trimeric MHA_2 in the absence of detergent (203 kDa). This difference is not surprising, since membrane proteins generally bind between 100 and 200 mol of detergent per mole of protein, adding between 50 and 100 kDa to the total molecular weight (*44*). Additionally, rodlike molecules, such as HA_2, have larger hydrodynamic radii than globular proteins and would be expected to run at a higher apparent molecular weight (*45*). The protein species is stable for weeks at 4 °C, as shown by reproducibility of the size-exclusion chromatogram, implying that the protein does not reaggregate once it is isolated in DM detergent micelles.

MHA_2 Is Stable in a Subset of Detergents. The 10 detergents that solubilized MHA_2 were tested for their abilities to maintain the protein in a homogeneous state. β-OG and DDM were tested by direct refolding. For other detergents, the protein was exchanged from DM into the test detergent by anion exchange chromatography and then purified by size-exclusion chromatography. The samples were examined by size-exclusion chromatography after one week to ensure protein stability. MHA_2 remained a trimer in four detergents (see Supporting Information). The commonly used detergent β-OG was found to be ineffective, while $C_{12}E_8$ was one of four detergents that successfully maintained the protein's elution profile by size-exclusion chromatography. Similar detergent-specific effects were seen in a study that examined reconstitution of full-length HA from virosomes, where it was found that viral envelopes could be functionally reconstituted when initially solubilized by $C_{12}E_8$ but not with β-OG (*46*). The other three stabilizing detergents, DM, UM, and Cymal-5, were all maltose-based detergents. Not surprisingly, chain length is an important variable, as the protein remains a homogeneous trimer in UM but not in DDM, even though the detergents only differ in size by one carbon unit. Maltoside detergents with shorter chains lengths (octyl and nonyl maltoside) do not solubilize the protein effectively.

Refolded MHA_2 Is a Trimer. Chemical cross-linking of MHA_2 results in three major bands on SDS−PAGE, the initial protein at just less than 70 kDa, a small amount of presumed dimer at 140 kDa, and a higher molecular weight band (Figure 3A). Since the top band runs at a larger molecular weight than expected, we carried out a control experiment with unreduced full-length HA, which is known to be trimeric and is of almost identical apparent molecular weight to MHA_2. The SDS−PAGE gel shows a similar pattern of three species (Figure 3B). The top bands for both MHA_2 and full-length HA probably represent the trimeric forms of the proteins. Linear migration of proteins by SDS−PAGE assumes fully denatured, single-chain polypeptides that are saturated by SDS, resulting in uniform hydrodynamic and charge characteristics (*47*). In this case, it is reasonable for these trimeric proteins run at a higher apparent molecular weight, due to their rodlike shapes and large sizes.

Given the limitations of using SDS−PAGE and size-exclusion chromatography for the accurate measurement of molecular weights, we used sedimentation equilibrium analytical ultracentrifugation (AUC) to determine the molecular weight and confirm the trimerization of MHA_2. For membrane proteins solubilized in detergent, however, determination of molecular weight by AUC is not trivial, as the amount of bound detergent and its partial specific volume is generally unknown. We approached this problem in two different ways. First, sedimentation equilibrium measurements were performed in solvents of different densities, and the data were analyzed using the density-modification method of Edelstein and Schachman (*34*, *35*). In this way, both the molecular weight and partial specific volume ($\bar{v}$) of the protein−detergent complex as well as the detergent micelle can be determined. All data were well described by a model reflecting a single sedimenting species, and buoyant molecular weight was a linear function of solvent density (Figure 4). Analysis of the data (see Methods) yielded a molecular mass of 263 ± 16 kDa for the protein plus detergent and a molecular mass of 37.9 ± 5.6 kDa for the DM detergent micelle alone. The amount of detergent bound per trimer is unknown; if we assume it is equal to the amount in a detergent micelle, the molecular mass for a single trimer is 225 ± 17 kDa. The amount of detergent associated with a membrane protein need not necessarily be equal to the amount present in a micelle. Indeed, it can vary greatly depending on the protein being studied, due to differences in hydrophobic surface area, and usually a larger amount of detergent is needed to solubilize a membrane protein than is present in micelles of pure detergent (*44*). Our data suggest that approximately 60 ± 16 kDa of DM bind per MHA_2 trimer, or the equivalent of 124 ± 33 mol of detergent per mole of trimer. The partial specific volumes of the protein plus detergent and the DM detergent micelle were determined to be 0.74 ± 0.01 and 0.76 ± 0.03 g/mL, respectively.

The second AUC method used takes advantage of a "neutrally buoyant" detergent. For a membrane protein with bound detergent, if the detergent and buffer are chosen such that the product of the partial specific volume of the detergent and the density are close to one, then the contribution of the bound detergent to the buoyant molecular weight is negligible. One such "neutrally buoyant" detergent is pentaoxyethylene octyl ether (C_8E_5), which has a $\bar{v}$ of 0.993 mL/g at 25 °C (*37*). As the density of most biochemical buffers is slightly greater than 1 at 25 °C, C_8E_5 is an excellent detergent for achieving neutral-buoyancy. Most recently, C_8E_5 has been used for examining the oligomerization of membrane-spanning α-helices (*36*, *48*). MHA_2 does not remain a homogeneous trimer in C_8E_5, as a small amount of aggrega-

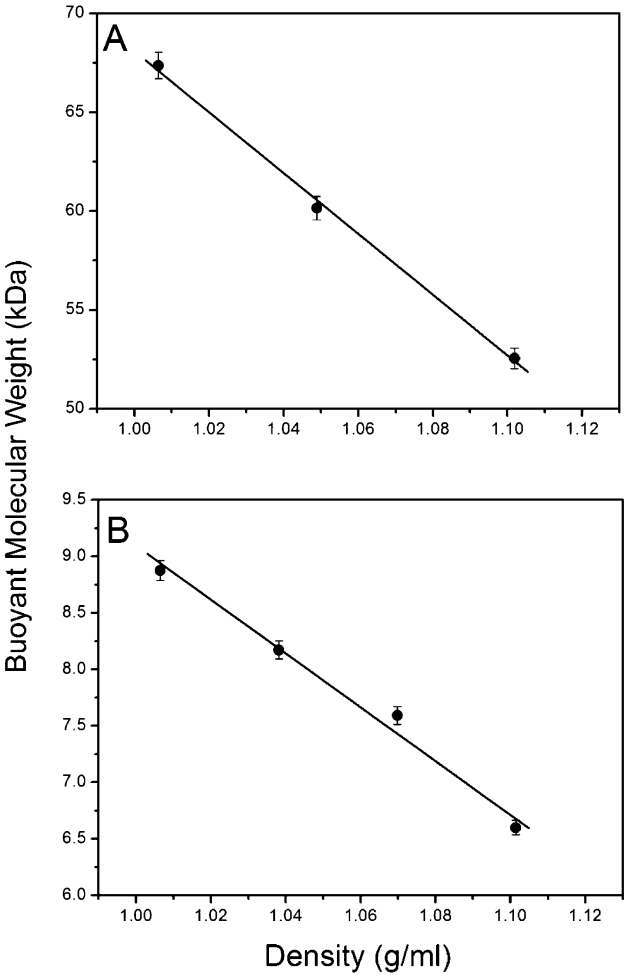

FIGURE 4: Buoyant molecular weight as function of solvent density for (A) MHA_2+DM and (B) DM alone. As described in the methods, each point represents a molecular weight determination from global analysis of multiple sedimentation equilibrium analytical ultracentrifugation datasets varying concentration and/or rotor speed. Solvent density was modified with D_2O, which, as expected from eq 2, results in a linear change in buoyant molecular weight. The measurement of buoyant molecular weight at multiple solvent densities allows determination of the molecular weight and partial specific volume of the sedimenting particle as described in the methods.

tion occurs over time, and we note that aggregation has been observed for other membrane protein systems solubilized in C_8E_5 studied by sedimentation equilibrium (*36*).

Figure 5 shows three representative analytical ultracentrifugation datasets for MHA_2 obtained using this method. For this experiment, protein prepared in DM was chromatographically exchanged into 20 mM sodium phosphate (pH 7.0), 200 mM NaCl, and 12 mM C_8E_5. The density for this solvent is 1.0075 at 25 °C (*31*), thus the product $\bar{v}\rho$ is 1 within the precision of the analytical ultracentrifuge. Global analysis of nine datasets taken at three different loading concentrations and three rotor speeds indicated that the results could not be attributed to a single sedimenting species or a monomer−dimer or higher-order association reaction. The best fit was obtained with a model describing two noninteracting species, a major component with a molecular mass of 197 ± 17 kDa and a minor species of 313 ± 36 kDa. The fitted values for the reference concentrations of the 197 kDa component were always 10−20-fold higher than the reference concentrations of the 313 kDa component. We

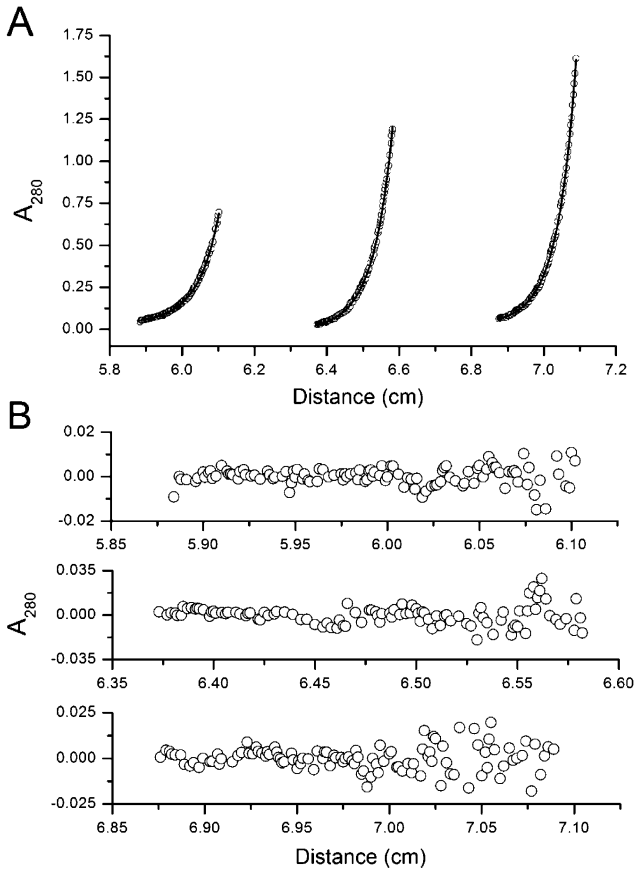

FIGURE 5: Sedimentation equilibrium analytical ultracentrifugation of MHA_2 in C_8E_5 under neutrally buoyant conditions. (A) Raw data for three concentrations spanning the range 0.12−0.5 mg/mL from a six-channel cell at 12 000 rpm. Solid line represents a fit to a model describing two noninteracting species as discussed in the text. (B) Residuals for the three datasets shown in A.

attribute the higher molecular weight component to a small amount of soluble aggregate (the exact amount of this component cannot be determined, as its extinction coefficient is unknown, but we estimate its presence to be ≤5%). Therefore, despite starting with chromatographically purified trimeric protein, aggregation of the protein solubilized in C_8E_5 occurred during the centrifugation experiment, as expected from the size-exclusion chromatography results. The major component of 197 ± 17 kDa is in reasonably good agreement with the expected molecular mass of 203 kDa for the MHA_2 trimer.

MHA_2 Is in the Low-pH Conformation. To ascertain whether MHA_2 is in the same conformation as the low-pH-induced form of HA_2, we used two monoclonal antibodies that recognize the low-pH-induced form but not the neutral-pH conformation of HA (*12*). The first, IIF4, which recognizes the low-pH form of HA_2 between residues 127 and 175, was used in a sandwich ELISA assay (Table 1). MHA_2 binds to the IIF4-coated plates regardless of pH treatment, while BHA only binds after incubation at low pH. These data indicate that the refolded MHA_2 is in the low-pH conformation at both pH 5 and pH 7, similar to ectodomain fragments of HA_2 produced in *E. coli*. (*13*, *14*).

The second monoclonal antibody, LC89, recognizes the turn (residues 106−112) between the long and short α-helices of the low pH-induced form of HA_2. Under the electron microscope, MHA_2 in the presence of DM appears as a long

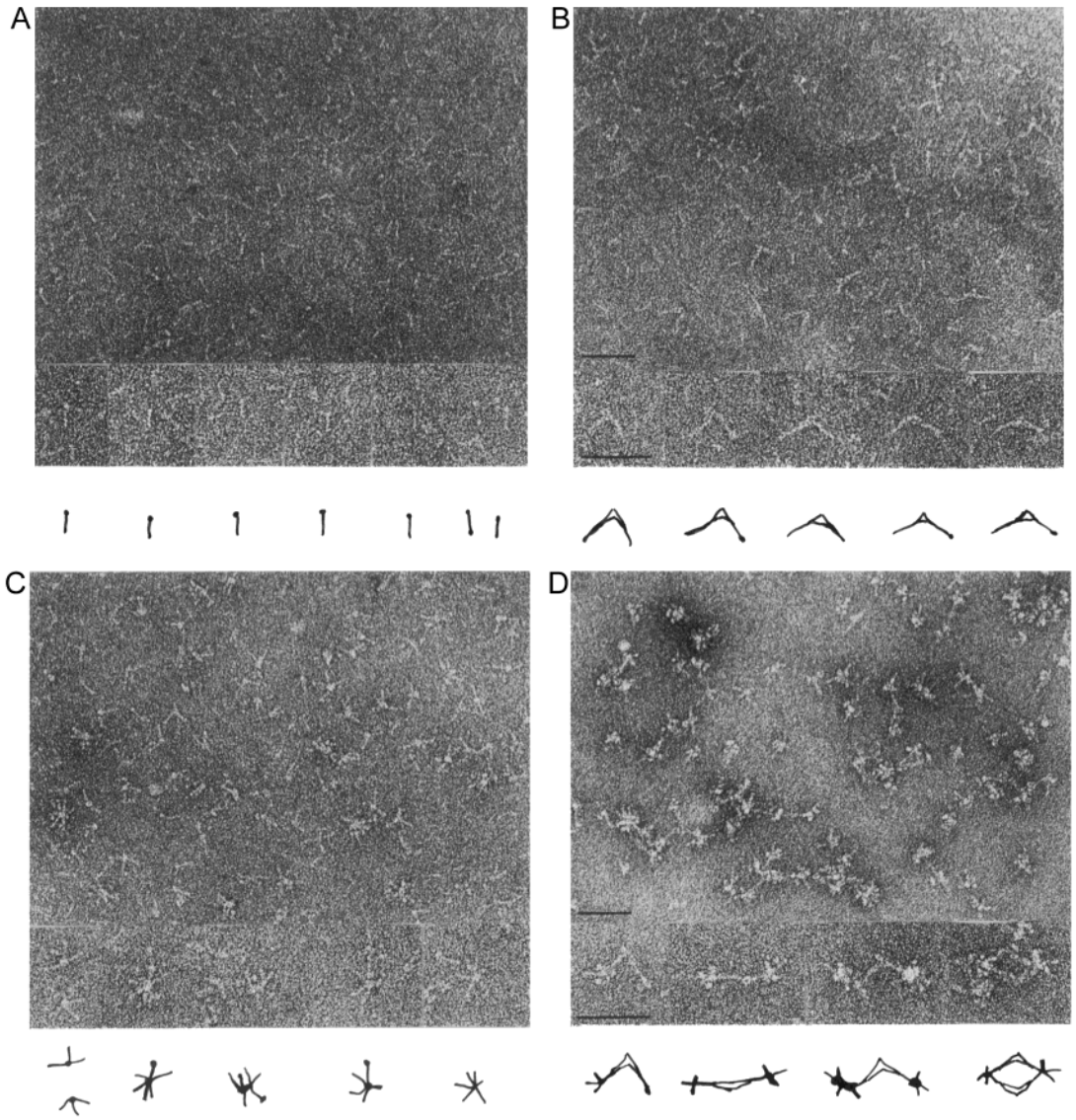

FIGURE 6: Electron micrographs of detergent-solubilized MHA_2 (A) alone, showing long rods with knobs at one end and (B) in complex with LC89 monoclonal antibody, which binds at one end of the rods. In the absence of detergent, the protein aggregates, as seen in micrographs (C) of the protein alone and (D) of protein in complex with LC89 monoclonal antibody. Representations of single molecules are shown below each micrograph. Bars = 50 nm.

Table 1: Antigenic Properties of BHA and MHA_2 at Neutral and Low pH[a]

protein	no primary mAb	anti-HA VACC	anti-MBP
BHA, pH 7	0.002 ± 0.002	0.02 ± 0.02	0.004 ± 0.003
BHA, pH 5	0.002 ± 0.002	0.7 ± 0.3	0.01 ± 0.01
MHA_2, pH 7	0.002 ± 0.002	0.7 ± 0.3	0.7 ± 0.3
MHA_2, pH 5	0.001 ± 0.001	0.5 ± 0.2	0.7 ± 0.2

[a] Antibody binding was estimated by ELISA using plates coated with anti-HA_2 IIF4 mAb. Absorption intensities were measured at 410 nm and were normalized to the strongest absorption on each plate. Values and sample standard deviations are measured from at least two separate experiments, each done in triplicate. The assays were performed at 22 °C at in the presence PBS, pH 7.4.

rod with a knob at one end of some of the molecules (Figure 6A) as is seen with both viral $TBHA_2$ and bacterially produced $EBHA_2$ (HA_2-38−175, Figure 1) (*12*, *14*). The majority of the rods has a length of 15.9 ± 1.5 nm, quite similar to the length of aggregated viral BHA_2 in rosettes, 15 nm (*49*). A subset (<20%) of the population has a length of 12.5 ± 1.0 nm, similar to $TBHA_2$ (11 nm) and $EBHA_2$ (12.4 nm) (*12*, *14*). It is not known why some of the rods appear shorter, but the presence of detergent may make hydrophobic regions less easily visible under the staining conditions used. When incubated with LC89, rods bound at one end by antibody are observed (Figure 6B). When MHA_2 is diluted in PBS the detergent concentration is reduced and the rods aggregate. The protein form rosettes with large centers, from which spikes of various lengths protrude, similar to full-length HA_2 rosettes (*49*). The longest spikes are 14.9 ± 0.8 nm to the center of the rosette with the protruding portion measuring 12.7 ± 0.6 nm (Figure 6C). The formation of rosettes with spikes of the given lengths suggests that the majority of soluble rods are significantly longer than both $TBHA_2$ and $EBHA_2$ due to the presence of the TM and MBP regions. Additionally, LC89 binds to the projected ends of the aggregated spikes (Figure 6D), consistent with the interpretation that the aggregation occurs via the TM region, at the opposite end of the rod from the LC89 binding site. Combined, the ELISA and EM data support the proposal that MHA_2 folds at neutral pH into the

same stable triple-stranded conformation as low-pH-induced HA_2 obtained from viral HA.

CONCLUSIONS

The increasingly detailed picture that we now have of events accompanying fusion by influenza virus HA still lacks several crucial elements. One is the conformation of the fusion peptide and the nature of its insertion into the target membrane. A second is the disposition of the transmembrane anchors in the viral membrane. A third is the relationship between these two hydrophobic segments when the conformational change is complete. Previous attempts to address these questions have involved fragments of protein outside the context of the full-length trimeric molecule. All three questions might be answered by visualization of the rearranged (postfusion) structure of HA_2 with these segments present, stabilized by detergent or lipid. Expression of full-length HA_2 that can be refolded into a stable trimer in the low-pH state allows us to do structural work using electron microscopy and X-ray crystallography and to undertake detailed mutagenesis studies of the HA_2 fusion peptide. Moreover, the fact that full-length HA_2 adopts the low-pH-induced conformation when produced through a refolding process at neutral pH provides further evidence for the notion that this conformation, seen first in the crystal structure of $TBHA_2$, is the thermodynamically preferred form of the protein.

ACKNOWLEDGMENT

The remaining authors acknowledge the mentorship, integrity, and enthusiasm of the late Don C. Wiley (1944−2001). We thank Ildem Akerman for help with detergent screening, Eva Vareckova for antibody IIF4, Qinghua Wang and Ya Ha for helpful discussions, and Kelly Arnett for assistance with the manuscript.

SUPPORTING INFORMATION AVAILABLE

A table describing the capabilities of the tested detergents to solubilize and maintain MHA_2 in a homogeneous state is provided. This material is available free of charge via the Internet at http://pubs.acs.org.

REFERENCES

1. Skehel, J. J., and Wiley, D. C. (1998) Coiled coils in both intracellular vesicle and viral membrane fusion. *Cell 95*, 871−4.
2. Skehel, J. J., and Wiley, D. C. (2000) Receptor binding and membrane fusion in virus entry: the influenza hemagglutinin. *Annu. Rev. Biochem. 69*, 531−69.
3. Eckert, D. M., and Kim, P. S. (2001) Mechanisms of viral membrane fusion and its inhibition. *Annu. Rev. Biochem. 70*, 777−810.
4. Wiley, D. C., and Skehel, J. J. (1987) The structure and function of the hemagglutinin membrane glycoprotein of influenza virus. *Annu. Rev. Biochem. 56*, 365−94.
5. Skehel, J. J., Bayley, P. M., Brown, E. B., Martin, S. R., Waterfield, M. D., White, J. M., Wilson, I. A., and Wiley, D. C. (1982) Changes in the conformation of influenza virus hemagglutinin at the pH optimum of virus-mediated membrane fusion. *Proc. Natl. Acad. Sci. U.S.A. 79*, 968−72.
6. Ruigrok, R. W. H., Martin, S. R., Wharton, S. A., Skehel, J. J., Bayley, P. M., and Wiley, D. C. (1986) Conformational changes in the hemagglutinin of influenza virus which accompany heat-induced fusion of virus with liposomes. *Virology 155*, 484−97.
7. Wilson, I. A., Skehel, J. J., and Wiley, D. C. (1981) Structure of the haemagglutinin membrane glycoprotein of influenza virus at 3 Å resolution. *Nature 289*, 366−73.
8. Carr, C. M., and Kim, P. S. (1993) A spring-loaded mechanism for the conformational change of influenza hemagglutinin. *Cell 73*, 823−32.
9. Bullough, P. A., Hughson, F. M., Skehel, J. J., and Wiley, D. C. (1994) Structure of influenza haemagglutinin at the pH of membrane fusion. *Nature 371*, 37−43.
10. Durrer, P., Galli, C., Hoenke, S., Corti, C., Gluck, R., Vorherr, T., and Brunner, J. (1996) H+-Induced membrane insertion of influenza-virus hemagglutinin involves the HA2 amino-terminal fusion peptide but not the coiled-coil region. *J. Biol. Chem. 271*, 13417−21.
11. Weber, T., Paesold, G., Galli, C., Mischler, R., Semenza, G., and Brunner, J. (1994) Evidence for H+-induced insertion of influenza hemagglutinin HA2 N-terminal segment into viral membrane. *J. Biol. Chem. 269*, 18353−8.
12. Wharton, S. A., Calder, L. J., Ruigrok, R. W. H., Skehel, J. J., Steinhauer, D. A., and Wiley, D. C. (1995) Electron microscopy of antibody complexes of influenza virus haemagglutinin in the fusion pH conformation. *EMBO J. 14*, 240−6.
13. Chen, J., Skehel, J. J., and Wiley, D. C. (1999) N- and C-terminal residues combine in the fusion-pH influenza hemagglutinin HA(2) subunit to form an N cap that terminates the triple-stranded coiled coil. *Proc. Natl. Acad. Sci. U.S.A. 96*, 8967−72.
14. Chen, J., Wharton, S. A., Weissenhorn, W., Calder, L. J., Hughson, F. M., Skehel, J. J., and Wiley, D. C. (1995) A soluble domain of the membrane-anchoring chain of influenza virus hemagglutinin (HA2) folds in *Escherichia coli* into the low-pH-induced conformation. *Proc. Natl. Acad. Sci. U.S.A. 92*, 12205−9.
15. Carr, C. M., Chaudhry, C., and Kim, P. S. (1997) Influenza hemagglutinin is spring-loaded by a metastable native conformation. *Proc. Natl. Acad. Sci. U.S.A. 94*, 14306−13.
16. Gething, M. J., Doms, R. W., York, D., and White, J. M. (1986) Studies on the mechanism of membrane fusion: site-specific mutagenesis of the hemagglutinin of influenza virus. *J. Cell Biol. 102*, 11−23.
17. Steinhauer, D. A., Wharton, S. A., Skehel, J. J., and Wiley, D. C. (1995) Studies of the membrane fusion activities of fusion peptide mutants of influenza virus hemagglutinin. *J. Virol. 69*, 6643−51.
18. Qiao, H., Armstrong, R. T., Melikyan, G. B., Cohen, F. S., and White, J. M. (1999) A specific point mutant at position 1 of the influenza hemagglutinin fusion peptide displays a hemifusion phenotype. *Mol. Biol. Cell 10*, 2759−69.
19. Han, X., Bushweller, J. H., Cafiso, D. S., and Tamm, L. K. (2001) Membrane structure and fusion-triggering conformational change of the fusion domain from influenza hemagglutinin. *Nat. Struct. Biol. 8*, 715−20.
20. Wharton, S. A., Martin, S. R., Ruigrok, R. W. H., Skehel, J. J., and Wiley, D. C. (1988) Membrane fusion by peptide analogues of influenza virus haemagglutinin. *J. Gen. Virol. 69*, 1847−57.
21. Han, X., and Tamm, L. K. (2000) A host−guest system to study structure−function relationships of membrane fusion peptides. *Proc. Natl. Acad. Sci. U.S.A. 97*, 13097−102.
22. Korte, T., Epand, R. F., Epand, R. M., and Blumenthal, R. (2001) Role of the Glu residues of the influenza hemagglutinin fusion peptide in the pH dependence of fusion activity. *Virology 289*, 353−61.
23. Tamm, L. K. (2003) Hypothesis: spring-loaded boomerang mechanism of influenza hemagglutinin-mediated membrane fusion. *Biochim. Biophys. Acta 1614*, 14−23.
24. Kemble, G. W., Danieli, T., and White, J. M. (1994) Lipid-anchored influenza hemagglutinin promotes hemifusion, not complete fusion. *Cell 76*, 383−91.
25. Roth, M., Doyle, C., Sambrook, J., and Gething, M. (1986) Heterologous transmembrane and cytoplasmic domains direct functional chimeric influenza virus hemagglutinins into the endocytic pathway. *J. Cell Biol. 102*, 1271−83.
26. Schroth-Diez, B., Ponimaskin, E., Reverey, H., Schmidt, M. F. G., and Herrmann, A. (1998) Fusion activity of transmembrane and cytoplasmic domain chimeras of the influenza virus glycoprotein hemagglutinin. *J. Virol. 72*, 133−41.
27. Melikyan, G. B., Lin, S., Roth, M. G., and Cohen, F. S. (1999) Amino acid sequence requirements of the transmembrane and cytoplasmic domains of influenza virus hemagglutinin for viable membrane fusion. *Mol. Biol. Cell 10*, 1821−36.
28. Armstrong, R. T., Kushnir, A. S., and White, J. M. (2000) The transmembrane domain of influenza hemagglutinin exhibits a

stringent length requirement to support the hemifusion to fusion transition. *J. Cell Biol. 151*, 425−37.
29. Gill, S. C., and von Hippel, P. H. (1989) Calculation of protein extinction coefficients from amino acid sequence data. *Anal. Biochem. 182*, 319−26.
30. Garboczi, D. N., Utz, U., Ghosh, P., Seth, A., Kim, J., VanTienhoven, E. A., Biddison, W. E., and Wiley, D. C. (1996) Assembly, specific binding, and crystallization of a human TCR-alphabeta with an antigenic Tax peptide from human T lymphotropic virus type 1 and the class I MHC molecule HLA-A2. *J. Immunol. 157*, 5403−10.
31. Laue, T. M., Shah, B., Ridgeway, T. M., and Pelletier, S. L. (1992) in *Analytical Ultracentrifugation in Biochemistry and Polymer Science* (Harding, S. E., Rowe, A. J., and Horton, J. C., Eds.) pp 90−125, Royal Society of Chemistry, Cambridge.
32. Cohn, E. J., and Edsall, J. T. (1943) in *Proteins, Amino Acids and Peptides* (Cohn, E. J., and Edsall, J. T., Eds.) pp 370−81, Reinhold Publishing Corporation, New York.
33. Bevington, P. R., and Robinson, D. K. (1992) *Data Reduction and Error Analysis for the Physical Sciences*, 2nd ed., McGraw-Hill, New York.
34. Edelstein, S. J., and Schachman, H. K. (1967) The simultaneous determination of partial specific volumes and molecular weights with microgram quantitites. *J. Biol. Chem. 242*, 306−11.
35. Edelstein, S. J., and Schachman, H. K. (1973) Measurement of partial specific volume by sedimentation equilibrium in H_2O−D_2O solutions. *Methods Enzymol. 27*, 82−98.
36. Fleming, K. G., Ackerman, A. L., and Engelman, D. M. (1997) The effect of point mutations on the free energy of transmembrane α-helix dimerization. *J. Mol. Biol. 272*, 266−75.
37. Ludwig, B., Grabo, M., Gergor, I., Lustig, A., Regenass, M., and Rosenbusch, J. P. (1982) Solubilized cytochrome *c* oxidase from *Paracoccus denitrificans* is a monomer. *J. Biol. Chem. 257*, 5576−8.
38. Chen, J., Skehel, J. J., and Wiley, D. C. (1998) A polar octapeptide fused to the N-terminal fusion peptide solubilizes the influenza virus HA2 subunit ectodomain. *Biochemistry 37*, 13643−9.
39. Maina, C. V., Riggs, P. D., Grandea, A. G. 3rd, Slatko, B. E., Moran, L. S., Tagliamonte, J. A., McReynolds, L. A., and de Guan, C. (1988) An *Escherichia coli* vector to express and purify foreign proteins by fusion to and separation from maltose-binding protein. *Gene 74*, 365−73.
40. Kapust, R. B., and Waugh, D. S. (1999) *Escherichia coli* maltose-binding protein is uncommonly effective at promoting the solubility of polypeptides to which it is fused. *Protein Sci. 8*, 1668−74.
41. Kobe, B., Center, R. J., Kemp, B. E., and Poumbourios, P. (1999) Crystal structure of human T cell leukemia virus type 1 gp21 ectodomain crystallized as a maltose-binding protein chimera reveals structural evolution of retroviral transmembrane proteins. *Proc. Natl. Acad. Sci. U.S.A. 96*, 4319−24.
42. Steinhauer, D. A., Wharton, S. A., Wiley, D. C., and Skehel, J. J. (1991) Deacylation of the hemagglutinin of influenza A/Aichi/2/68 has no effect on membrane fusion properties. *Virology 184*, 445−8.
43. Nominé, Y., Ristriani, T., Laurent, C., Lefèvre, J.-F., Weiss, É., and Travé, G. (2001) Formation of soluble inclusion bodies by HPV E6 oncoprotein fused to maltose-binding protein. *Protein Expr. Purif. 23*, 22−32.
44. Moller, J. V., and le Maire, M. (1993) Binding as a measure of hydrophobic surface area of integral membrane proteins. *J. Biol. Chem. 268*, 18659−72.
45. Stellwagen, E. (1990) Gel filtration. *Methods Enzymol. 182*, 317−28.
46. Stegmann, T., Morselt, H. W. M., Booy, F. P., van Breemen, J. F. L., Scherphof, G., and Wilschut, J. (1987) Functional reconstitution of influenza virus envelopes. *EMBO J. 6*, 2651−9.
47. Garfin, D. E. (1990) One-dimensional gel electrophoresis. *Methods Enzymol. 182*, 425−41.
48. Fleming, K. G., and Engelman, D. M. (2001) Specificity in transmembrane helix-helix interactions can define a hierarchy of stability for sequence variants. *Proc. Natl. Acad. Sci. U.S.A. 98*, 14340−4.
49. Ruigrok, R. W. H., Wrigley, N. G., Calder, L. J., Cusack, S., Wharton, S. A., Brown, E. B., and Skehel, J. J. (1986) Electron microscopy of the low pH structure of influenza virus haemagglutinin. *EMBO J. 5*, 41−9.

BI049807K